Mol Breeding (2023) 43:66
https://doi.org/10.1007/s11032-023-01410-3

Mapping QTL conferring flag leaf senescence in durum wheat cultivars

Yan Ren · Xiaonan Sun · Jingyun Nie · Peng Guo · Xiaohui Wu · Yixiao Zhang · Mengjuan Gao · Mohsin Niaz · Xia Yang · Congwei Sun · Ning Zhang · Feng Chen

Received: 14 April 2023 / Accepted: 17 July 2023 / Published online: 8 August 2023

Abstract Flag leaf senescence is a critical factor affecting the yield and quality of wheat. The aim of this study was to identify QTLs associated with flag leaf senescence in an F_{10} recombinant inbred line population derived from durum wheats UC1113 and Kofa. Bulked segregant analysis using the wheat 660K SNP array identified 3225 SNPs between extreme-phenotype bulks, and the differential SNPs were mainly clustered on chromosomes 1A, 1B, 3B, 5A, 5B, and 7A. BSR-Seq indicated that the significant SNPs were mainly located in two intervals of 354.0–389.0 Mb and 8.0–15.0 Mb on 1B and 3B, respectively. Based on the distribution of significant SNPs on chromosomes 1B and 3B, a total of 109 insertion/deletion (InDel) markers were developed, and 8 of them were finally used to map QTL in UC1113/Kofa population for flag leaf senescence. Inclusive composite interval mapping identified two major QTL in marker intervals Mar2005–Mar2116 and Mar207–Mar289, explaining 14.2–15.4% and 31.4–68.6% of the phenotypic variances across environments, respectively. Using BSR-Seq, gene expression and sequence analysis, the TraesCS1B02G211600 and TraesCS3B02G023000 were identified as candidate senescence-associated genes. This study has potential to be used in cloning key genes for flag leaf senescence and provides available molecular markers for genotyping and marker-assisted selection breeding.

Keywords Durum wheat · Flag leaf senescence · Molecular marker · Linkage mapping

Introduction

Durum (*Triticum turgidum* subsp. *durum* (Desf.) Husnot) and bread wheat (*Triticum aestivum* L.) provide roughly 20% of the calories consumed by humans and are crucial to global food security (Li et al. 2021). Flag leaves are one of important photosynthetic organs of wheat, play an important role in determining the grain yield of wheat. It has been reported that almost 50% of the assimilates for grain filling are derived from the photosynthates of the flag leaf (Liu et al. 2018). In wheat, flag leaf senescence (FLS) relates to the period of reallocating resources from the source to the sink during grain filling (Verma et al. 2004). The appropriate initiation and progression of FLS are essential for improving wheat yield potential (Uauy et al. 2006a). Generally, leaf senescence,

Supplementary Information The online version contains supplementary material available at https://doi.org/10.1007/s11032-023-01410-3.

Y. Ren · X. Sun · J. Nie · P. Guo · X. Wu · Y. Zhang · M. Gao · M. Niaz · X. Yang · C. Sun · N. Zhang · F. Chen (✉)
National Key Laboratory of Wheat and Maize Crop Science/Agronomy College/CIMMYT-China Wheat and Maize Joint Research Center, Henan Agricultural University, Zhengzhou 450046, China
e-mail: fengchen@henau.edu.cn

the last stage of leaf development, is controlled by an innate genetic program including age, phytohormones, reactive oxygen species (ROS), and reproduction (Gan and Amasino 1995; Beers and McDowell 2001; Lim et al. 2007; Woo et al. 2013). Moreover, leaf senescence can also be triggered by unfavorable environmental stresses during leaf development (Leng et al. 2017; Hu et al. 2017; Woo et al. 2019). Senescence is characterized by a series of changes in cellular physiological and biochemical changes in leaf cells that ultimately boost reproductive success by redistributing resources to growing tissues or storage organs like flowers and seeds (Guo and Gan 2005; Lim et al. 2007). Efficient senescence is essential for maximizing viability in the next generation or season (Hörtensteiner and Feller 2002). However, premature leaf senescence caused by various internal or environmental signals reduces the yield of major cereal grains, such as rice, maize, and wheat (Distelfeld et al. 2014).

In model plants such as *Arabidopsis*, tomato, and rice, a large collection of genes involved in the regulation of leaf senescence was identified through forward genetics and multi-omics approach (Lim et al. 2007; Woo et al. 2013; Kim et al. 2016; Woo et al. 2016; Li et al. 2020b; Xiong et al. 2021). Through high-throughput DNA microarray analysis, more than 800 genes were identified as senescence-associated genes (SAGs) in *Arabidopsis*. Recent studies suggested that temporal regulation of transcription factors, including those in the WRKY (contains the WRKY amino acid signature at the N-terminus and a novel zinc-finger structure at the C-terminus) and NAC (NAM, ATAF, and CUC) families (Olsen et al. 2005; Rushton et al. 2010), is critical for cascades of biological changes in the progression of leaf senescence or FLS (Lim et al. 2007; Kim et al. 2016; Lei et al. 2022; Cohen et al. 2022). Using the combination of transcriptomic and forward genetic approaches, the functions and processes of melatonin in controlling leaf senescence have been demonstrated in rice (Liang et al. 2015). In addition, the construction of various senescence mutants has provided important information for understanding hundreds of functional SAGs (Li et al. 2020b).

Durum wheat contributes to wheat primary gene pool and is cultivated on around 18 million ha worldwide with an annual production of approximately 35 million tons (Cakmak et al. 2010). Although FLS is a major factor affecting wheat production worldwide, a few studies have recently reported QTL and molecular markers for FLS in durum and bread wheat. Thus, it is essential to identify QTLs and genes associated with FLS in order to improve plant fitness and yield.

The wheat 660K SNP array and RNA-sequencing have been utilized successfully to identify genetic loci linked to quality traits, agronomic traits, and disease resistance in bread wheat (Zhang et al. 2017; Mu et al. 2019; Zhao et al. 2020; Li et al. 2022; Qu et al. 2022). A major stripe rust resistance QTL was mapped to a 0.4 cM genetic region on chromosome 7B using the wheat 600K SNP array to genotype bulked extremes (Mu et al. 2019). In addition, Qu et al. (2022) used bulked segregant analysis (BSA) and wheat 660K SNP array to rapidly identify genomic regions for kernel length and thousand-kernel weight of wheat. Moreover, the two major QTL for tiller angle were rapidly identified by BSR-Seq and the wheat 660K SNP array (Zhao et al. 2020). Using BSA-wheat 660K array and BSR-Seq technologies, two loci for black point resistance were also identified (Li et al. 2022). Due to the high proportion of shared alleles between tetraploid durum and hexaploidy bread wheat (Dvorak et al. 2006; Wang et al. 2014), the wheat 660K SNP array and resequencing data of bread wheat cultivars serve as invaluable resource for genotyping tetraploid durum wheat.

The objectives of this study were to (1) identify major genetic loci for FLS in a recombinant inbred line (RIL) population derived from two durum wheat cultivars UC1113 and Kofa, (2) develop molecular markers related to FLS for wheat breeding, and (3) identify candidate genes on chromosomes 1B and 3B through BSR-Seq and gene sequence.

Materials and methods

Plant materials

A F_{10} RIL population consisting of 93 lines was generated by single seed descent method from a cross of durum wheats UC1113 and Kofa. Kofa is a durum cultivar and has excellent pasta quality with optimal semolina and pasta color, high protein content, and strong gluten, whereas UC1113 is a durum accession from UC Davis wheat breeding program and has great excellent agronomic performance (Zhang et al. 2008).

UC1113 and Kofa both showed normal FLS timing in the field from 2018 to 2021 (Fig. S1), whereas the RILs in the UC1113/ Kofa (UK) population showed obvious differences of FLS timing. Subsequently, we evaluated FLS from the heading to milky stage of the UK population and parents at Zhengzhou in four years (2018, 2019, 2020, and 2021) and at Yuanyang, Henan province, in three years (2019, 2020, and 2021). The field trials were conducted in randomized complete blocks with two replications. Each accession was planted in two 1.5 m rows spaced 30 cm apart, with 15 seeds in each row. Field data from Yuanyang 2020–2021 was excluded from the statistical analysis and QTL detection due to the low FLS score.

We scored FLS in a scale of 0–4 based on the percentage of green flag leaf area (GFLA) as described in previous report (Verma et al. 2004) (Fig. 1A, B), where category 0: full green (100%); 1: the GFLA is more than 75%; 2: the GFLA is more than 50% and less than 75%; 3: the GFLA is more than 25% and less than 50%; 4: the GFLA is less than 25%. The FLS rating was recorded in every five days from approximately 25 days after flowering. The maximum FLS rating for each replication and the mean FLS rating of two replications were used for subsequent data analysis.

DNA extraction and BSA

Wheat flag leaves were collected from parents and RILs in the field at the beginning of May for extraction of genomic DNA using the sodium lauryl sulfate (SLS) method (Chen et al. 2011). Two normal senescence bulks (NSB) and two premature senescence bulks (PSB) were made by forming an equal amount

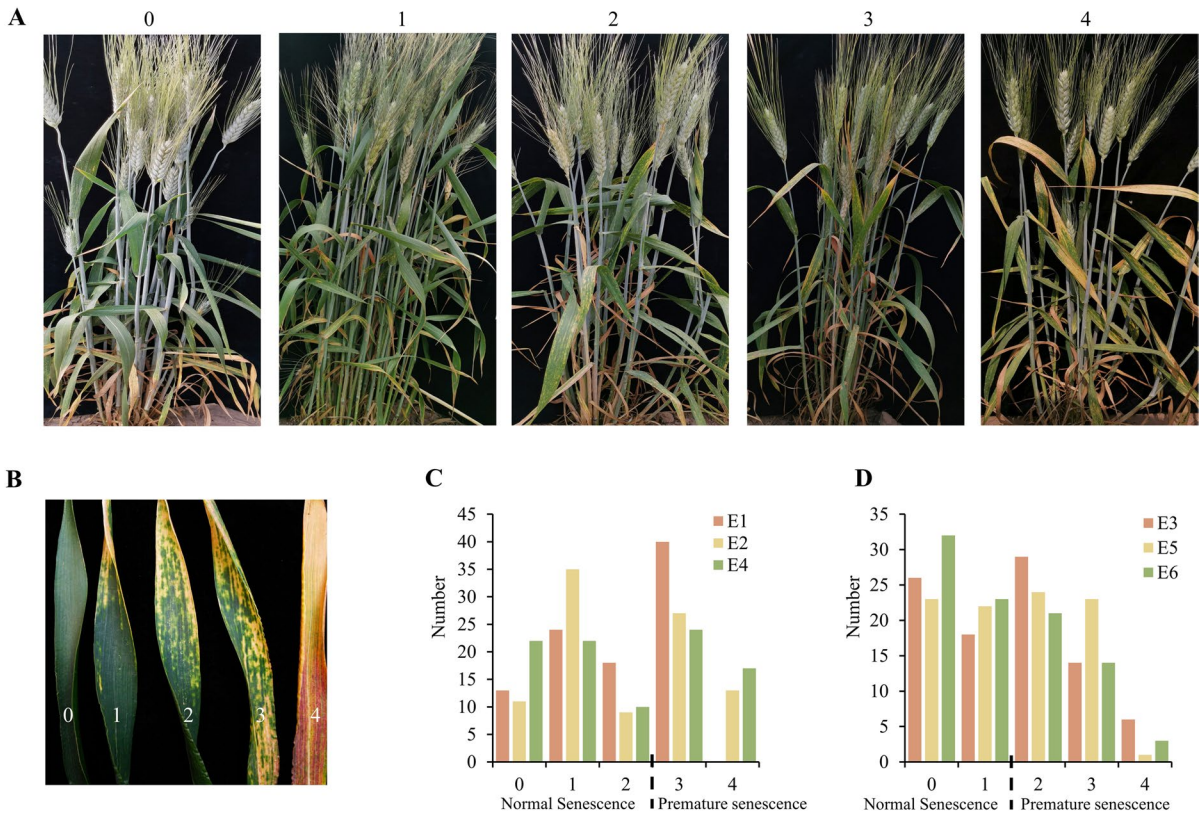

Fig. 1 Schematic diagram for phenotypic evaluation of flag leaf senescence (FLS) of lines (**A**) and leaves (**B**) in the field and the phenotypic distribution of 93 RILs into 5 categories based on response to FLS rating across six environments (**C, D**). 0, full green; 0–1, green flag leaf area (GFLA) >75%; 1–2, 75%>GFLA >50%; 2–3, 50%>GFLA>25%; 3-4, GFLA<25%. E1 to E6, Zhengzhou 2017–2018, Yuanyang 2018–2019, Zhengzhou 2018–2019, Yuangyang 2019–2020, Zhengzhou 2019–2020, and Zhengzhou 2020–2021 seasons, respectively. FLS refers to flag leaf senescence

of DNA from 10 RILs with normal senescence and 10 with premature senescence, respectively, based on their FLS scores (0 or 1 for NSB; 3 or 4 for PSB) in 2018 and 2019. The extreme-phenotype bulks were genotyped using the wheat 660K SNP array at China Golden Marker Biotech Co. Ltd. (Beijing, China). SNP genotyping and clustering were processed using Affymetrix Axiom Analysis Suite software (Thermo Fisher Scientific, Waltham, MA, USA). A dish QC (DQC) value ≥ 0.82 and call rate (CR) ≥ 95 were used as the criteria for SNP filtering (Baurley et al. 2016). The consistent SNPs between two NSB and two PSB were assumed to be associated with FLS.

BSR-Seq and molecular genotyping

In April 2020, the flag leaves of RILs for two NSB and two PSB were sampled and frozen immediately in liquid nitrogen for BSR-Seq. Total RNA was isolated using the TRIzol reagent (Invitrogen). RNA concentration and purity were measured using NanoDrop 2000 (Thermo Fisher Scientific, Wilmington, DE). RNA integrity was assessed using the RNA Nano 6000 Assay Kit of the Agilent Bioanalyzer 2100 system (Agilent Technologies, CA, USA). Sequencing library of each sample was constructed using an NEBNext UltraTM RNA Library Prep Kit for Illumina (NEB, USA) following the manufacturer's instructions.

SNP and InDel genotype calling were processed with GATK2 software. SNP/InDel filtering criteria were as follows: monomorphic and poor-quality SNP/InDel with more than 10% missing values, ambiguous calling, and minor allele frequencies < 5% were excluded from subsequent analysis. The SNPs between two NSB and two PSB were calculated by R program. The regions associated with potential FLS QTL were analyzed using four methods, including the SNP density method, VarScore algorithm method (Dong et al. 2020), Euclidean distance (ED) method (Hill et al. 2013), and SNP-index method (Takagi et al. 2013). The regions determined by four methods were considered candidate regions identified by BSR-Seq.

Differential expression analysis of two NSB and two PSB was performed using the DESeq2 which provides statistical routines for determining differential expression in digital gene expression data using a model based on the negative binomial distribution. The resulting *P* values were adjusted using the Benjamini and Hochberg's approach for controlling the false discovery rate. Genes with an adjusted *P* value < 0.05 found by DESeq2 were assigned as differentially expressed.

Development of InDel markers

Using wheat genome resequencing data of 480 bread wheat cultivars available in our lab, 232 polymorphic sites, including InDels, were found in the range of 354.0–389.0 Mb of chromosome 1B. Then the upstream and downstream sequences of these InDel loci were downloaded. Based on the interval distribution of SNPs, 32 primers were developed in the region using primer designing tool (https://www.ncbi.nlm.nih.gov/tools/primer-blast/index.cgi) and Primer3Plus software (https://www.primer3plus.com) (Table S1). After verifying the polymorphism between two NSB and two PSB, three polymorphic InDel markers (Mar2005, Mar2116, and Mar2128) with distinct physical positions were employed to genotype the UK population (Table 1; Fig. S2-D-F). Using the same method, 813 polymorphic sites, including InDels, were found in the interval of 8.0–15.0 Mb on chromosome 3B. Based on the interval distribution of SNPs on chromosome 3B (Fig. 3C), 32 InDel markers were developed within the 7 Mb region (Table S1). First, these InDel markers were tested on the two NSB and two PSB, five of them showing polymorphisms between the extreme bulks, and subsequently, three (Mar207, Mar289 and Mar311) with different physical positions were used to genotype the UK population (Table 1; Fig. S2-A-C). However, the results of QTL mapping showed that the LOD contours did not fall completely (Fig. S3). Hence, we further identified the polymorphic sites, including InDels in the range of 5.0–8.0 Mb and 15.0–20.0 Mb of chromosome 3B and their upstream and downstream sequences to further develop flanking markers, and eventually added one InDel marker on each side (Mar122 and Mar389), respectively (Table 1).

Map construction and QTL analysis

A total of 269 polymorphic SSR markers between UC1113 and Kofa were used to genotype the mapping population and construct a genetic map in a previous study (Zhang et al. 2008). These reported

Table 1 Indel markers mapped to genetic linkage map of chromosomes 1B and 3B and the specific primers for real-time PCR

Marker name	Forward primer (5′-3′)	Reverse primer (5′-3′)	Physical position (Mb)[a]	Annealing temperature (°C)	Fragment size (bp) NSL/PSL[b]	Description
Mar122	TCTCGCGTAGAA GATACAGAGC	ACTTACGGA GGCGCCAGAG	5.6	63	138/152	InDel marker
Mar207	GAGGAATTA CGGTGGGCC TTA	ACGAGGTGC CGAGATGGT AA	8.8	63	172/158	InDel marker
Mar289	GACTTCCTTGCT TTTCGTGC	GCGGGCTTC ACTAAAATCC	12.4	63	165/231	InDel marker
Mar311	TGTGCTAAG AGCCTGAGG GA	CCAACGCAC TCTACCACAGT	14.2	63	152/177	InDel marker
Mar389	CCGTGTACA AGGCAAGCGA	GATCTCCTGCCC GCCATC	18.7	63	135/127	InDel marker
Mar2005	AGCTACGTC GCGATCCAA AT	GCACACACA CGTAAACCC AG	359.2	63	124/142	InDel marker
Mar2116	CCAGGTTCAATG TATGTATTG TTGT	TATAAATCTAGT ACTCCCTCT CCCT	385.1	63	193/177	InDel marker
Mar2128	ATGTCTGAATGC GGCTTTGC	ACAGGTTAATTA GTGCTTCCGC	386.2	63	181/159	InDel marker
TraesCS3B02G020700	TCTCGGTCTCAC TCGCC	CTCCTTGAG CACCTTCACG	8.7	60	140	For real-time PCR
TraesCS3B02G021000	CCAAGTGCTACA TCCTCGAC	TGCAGGACA TTGAAGCCT TT	8.8	60	130	For real-time PCR
TraesCS3B02G021100	GCATCTTTGGTG GCTTGG	TTGGGGTGG AGGAGGG	8.8	60	164	For real-time PCR
TraesCS3B02G022500	CTGGCTTCCCCT TCTT	TCAGTCCAA ACTTTCTCG	9.7	60	222	For real-time PCR
TraesCS3B02G022600	CCTCCCTGACAC CTTCT	TCGTCCAGCCTT CCA	9.8	60	197	For real-time PCR
TraesCS3B02G023000	CTCCGCCACTTG TTCAGCA	CGCCAGCCA TGTGTCGA	9.9	60	225	For real-time PCR
TraesCS3B02G023400	CCCACGGCA GTTCAGACC	GCGATGGAG GACAAGTAA GGG	10	60	236	For real-time PCR
TraesCS3B02G024000	TGCTTCCTCATC TCCG	GCGTCTCCC TGCTTT	10.2	60	209	For real-time PCR
TraesCS3B02G024100	GACCAATCC ACCCTCCCTG	CGGTCAATG TTGCTCGCAG	10.3	60	239	For real-time PCR
TraesCS3B02G024200	ACGTCGGGT GCTTCA	ACTGCCAAA TCCATAACA	10.3	60	183	For real-time PCR
TraesCS1B02G207100	GCCCCGACT GCTTCT	ATGCCGTTG AGGACC	374.3	60	214	For real-time PCR
TraesCS1B02G211600	CCAAGCACA AGAACATAGT	CATTCAAGT CCGCAAGA	385.1	60	178	For real-time PCR

[a]Physical position, physical position of the Indel marker against the reference genome sequence of Chinese Spring (IWGSC, https://urgi.versailles.inra.fr/blastiwgsc/blast.php)

[b]NSL/PSL, normal senescence lines/premature senescence lines

polymorphic SSR markers and the filtered InDel markers were used to construct a new genetic map using the software IciMapping 4.1 (http://www.isbreeding.net) in the present study. Inclusive composite interval mapping (ICIM) with the ICIM-ADD function of the software IciMapping 4.1 was then used to map the QTL based on the FLS rating for each replicate and the means of two replicates in all environments. A LOD threshold of 2.5 was set for declaring significant QTL based on 1000 permutations at $P < 0.05$. QTL effects were estimated as the proportion of phenotypic variance explained (PVE) by the QTL. Physical positions of mapped markers in the QTL regions were obtained by blasting flanking sequences of InDels against the reference genome sequences of Chinese Spring (https://urgi.versailles.inra.fr/blast_iwgsc/blast.php).

qRT-PCR analysis

The qRT-PCR analysis was performed following Lv et al. (2021) with minor modifications. Relative expression levels were evaluated according to the relative quantification method $2^{-\Delta\Delta CT}$ (Livak and Schmittgen 2001). The expression levels of candidate genes were detected using specific primers (Table 1). The wheat *β-actin* gene (GenBank accession number: AB181991) was used as an internal control.

Statistical analysis

Phenotypic correlation coefficients and Student's *t*-test were conducted using the Excel software. Analysis of variance (ANOVA) was performed with the General Linear Model in the IBM SPSS Statistics 26.

Results

Flag leaf senescence distributed in the UK population

The mean FLS score was 0.3 for the parent Kofa and 0.2 for UC1113 across six environments. Bimodal distribution of FLS rating among 93 offspring lines ranged from 0 to 3.5 with a mean of 1.5 among six environments, indicating a significant difference among lines (Table S2; Fig. 1C, D). Pearson's correlation coefficients of FLS scores for the mapping population ranged from 0.745 to 0.958 among six environments ($P < 0.01$) (Table S3). ANOVA showed a significant variation among genotypes and genotype-environment interaction (G×E), but no significant between environments (Table S4).

Significant SNPs were detected to be associated with FLS by BSA

To map the genetic loci for FLS, we genotyped two NSB and two PSB using the wheat 660K SNP array. After filtering out SNPs with the criteria of DQC ≤ 0.82 and CR ≥ 95, we selected 226,737 high-resolution SNPs from the 660,014 SNPs for further analysis. A total of 3225 SNPs showed polymorphisms between two NSB and two PSB (Table S5). These SNPs were mainly located on chromosomes 1A, 1B, 3B, 5A, 5B, and 7A, which might be associated with FLS in the UK population (Fig. 2A). However, the candidate QTL region on these chromosomes was larger (Fig. 2B).

Two loci were detected to be associated with FLS by BSR-Seq analysis

We sequenced the transcriptomes of the aforementioned four extreme bulks. After quality control, a total of 219.1 Gb Clean Data with a minimum Q30 of 94.0% were obtained (Table S6). About 92.9% of reads were aligned to the Chinese Spring reference sequences, among which ~88.1% were uniquely mapped reads (Table S7). Based on the results by BSR-Seq, candidate regions associated with FLS in the UK population were identified on chromosomes 1B and 3B, which represented corresponding regions identified by all methods (Fig. 3A). The SNP density revealed that the majority of variations between two NSB and two PSB were mainly located between 283.0–284.0 Mb on 1B and 8.0–14.0 Mb on 3B (Table S8). Using the highest scoring points of the VarBScore algorithm, the candidate loci for FLS were located in similar regions of 281.0–286.3 Mb on 1B and 11.3–14.0 Mb on 3B (Table S9). The SNP-Index method found that 1B (37.7–389.7 Mb) and 3B (8.0–17.1 Mb and 416.6–418.1 Mb) were associated with FLS based on the chromosomal distributions of clustered polymorphic SNPs and InDels above 0.4 or under −0.4. On the basis of fitted ED^4 value above 1.0, two genetic loci for FLS were located within 192.3–389.1 Mb on 1B and 7.0–17.6 Mb on 3B.

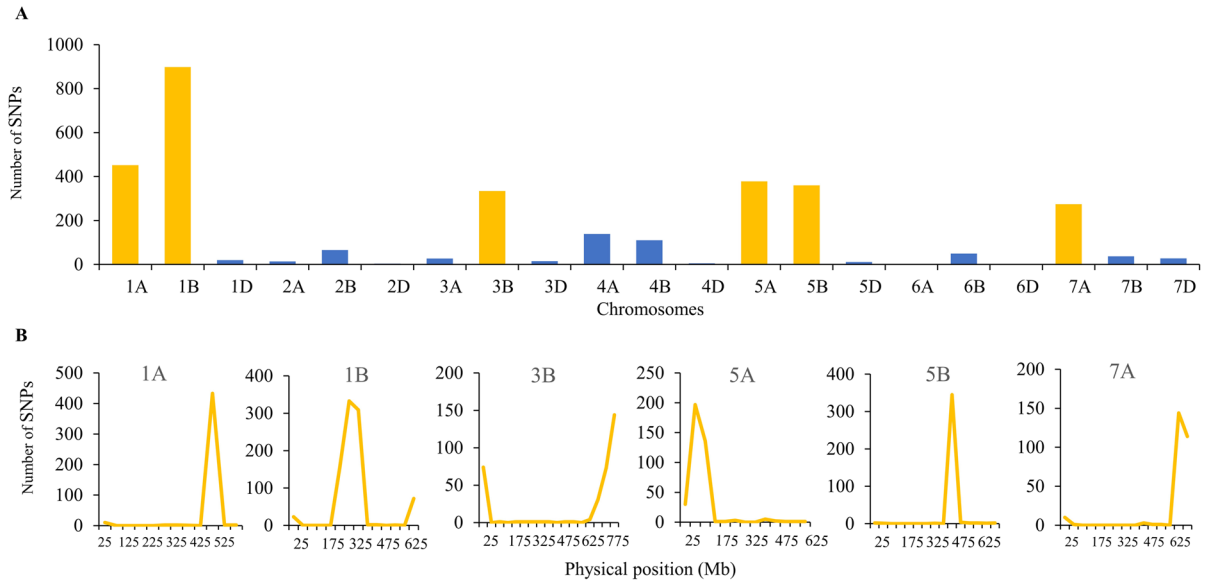

Fig. 2 Distribution of SNPs associated with flag leaf senescence (FLS) on all chromosomes (**A**) and the distribution of SNPs associated with FLS on chromosomes 1A, 1B, 3B, 5A, 5B, and 7A (**B**)

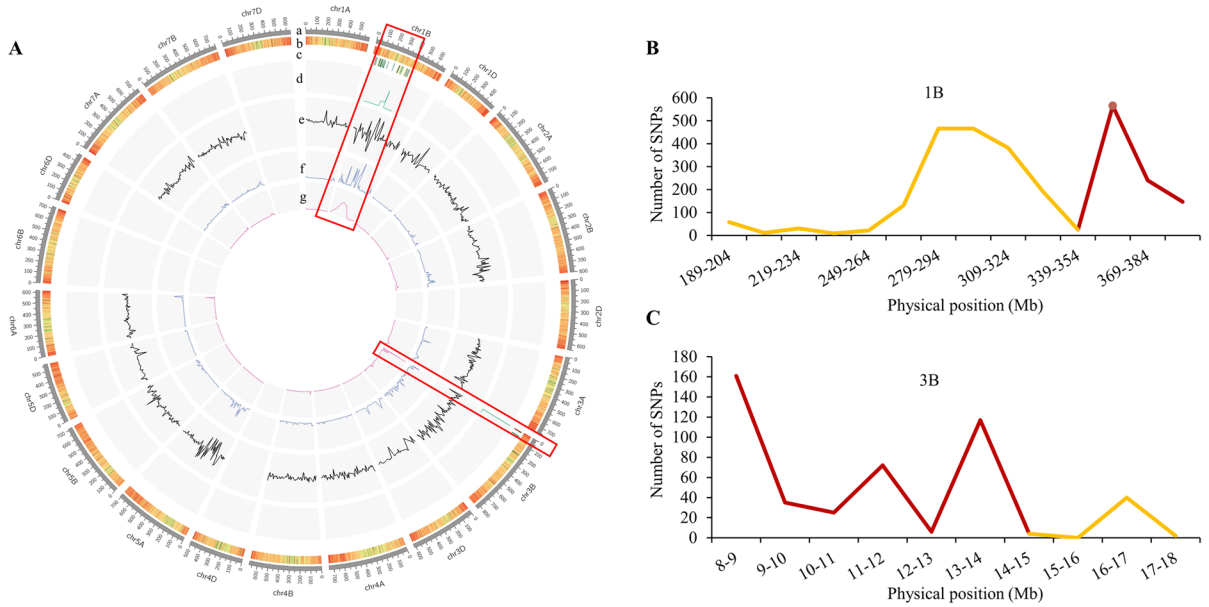

Fig. 3 Circles represent the molecular mapping for flag leaf senescence (FLS) by BSR-Seq analysis (**A**) and the distribution of SNPs associated with FLS on chromosomes 1B (**B**) and 3B (**C**) based on SNP densities, VarScore algorithm, Euclidean distance (ED) and SNP-index methods. a Chromosome scale plate, b Gene density (gene number/1Mb), c SNP density, d VarBScore, e SNP-index, f G value, and g fitted ED^4 value

Consequently, combining the above results, it is suggested that the candidate regions associated with FLS in the UK population were probably on chromosomes 1B (192.3–389.1 Mb) and 3B (8.0–17.1 Mb). Furthermore, the interval distribution of significant SNPs on chromosomes 1B and 3B was mostly concentrated

in the intervals of 354.0–389.0 Mb (Fig. 3B) and 8.0–15.0 Mb (Fig. 3C), respectively.

QTL mapping revealed two genetic loci for FLS

Integration of BSA-wheat 660K array and BSR-Seq showed that two important genetic loci for FLS were located on chromosomes 1B and 3B, respectively, which mainly concentrated in a 35 Mb region on 1B and a 7 Mb region on 3B according to Chinese Spring reference genome. Using the wheat resequencing data of 480 bread wheat cultivars available in our lab, the InDel variant loci in the intervals of the two loci were identified, and 8 additional polymorphic InDel markers were added in the targeting region. Combining the genotypes and FLS scores of RILs (Table S2; Table S10), the two major QTL for FLS, designated as *Q.FLS.hnau-1BL* (PVE=14.2%–15.4%) and *Q.FLS.hnau-3BS* (PVE=31.4%–68.6%), were mapped on chromosomes 1B and 3B, respectively (Table 2 and Fig. 4). The normal FLS alleles of *Q.FLS.hnau-1BL* and *Q.FLS.hnau-3BS* originated from the parent Kofa.

The effect of the two QTLs was further estimated based on their flanking InDel markers. Results showed that *Q.FLS.hnau-1BL* conferred 0.6–1.0 of reduced FLS scores, whereas *Q.FLS.hnau-3BS* reduced FLS scores by 1.8–2.4 in different environments (Table S11).

Candidate genes were predicted in *Q.FLS.hnau-1BL* and *Q.FLS.hnau-3BS*

Q.FLS.hnau-1BL was mapped in a 2.9 cM region between markers Mar2005 and Mar2116, from 359.2 Mb to 385.2 Mb based on the Chinese Spring reference genome (https://urgi.versailles.inra.fr/blast_iwgsc/), including 108 high-confidence annotated genes (TraesCS1B02G200500–TraesCS1B02G211600) in the interval. The BSR-Seq analysis showed that only TraesCS1B02G207100 and TraesCS1B02G211600 of the 108 annotation genes in Chinese Spring were significantly differentially expressed between two NSB and two PSB (Table S12). qRT-PCR results showed that the expression of TraesCS1B02G211600 was more significantly different between the normal and premature RILs (Fig. 5A). In addition, the results of gene sequencing results depicted that a 16-bp deletion (TTTCAGTGCTAGATACA/T) in the downstream of TraesCS1B02G211600 was significantly associated with FLS in the UK population. Based on these results, TraesCS1B02G211600 was considered a candidate SAG for *Q.FLS.hnau-1BL*.

Q.FLS.hnau-3BS was mapped between the markers Mar207 and Mar289, which defines a 3.6 Mb region in Chinese Spring (8.8–12.4 Mb). The candidate regions on chromosome 3B include 82 high-confidence annotated genes (TraesCS3B02G020700–TraesCS3B02G028900)

Table 2 QTLs associated with flag leaf senescence in the UC1113/Kofa RIL population

QTL name	Environment	LeftMarker	RightMarker	Position (cM)	Physical interval (Mb)[a]	LOD	PVE (%)[b]	Add[c]
Q.FLS.hnau-1BL	E2[d]	Mar2005	Mar2116	95	359.2–385.2	3.0	15.44	−0.45
	E3	Mar2005	Mar2116	95	359.2–385.2	3.2	15.00	−0.44
	E4	Mar2005	Mar2116	95	359.2–385.2	3.0	14.21	−0.50
	E5	Mar2005	Mar2116	95	359.2–385.2	3.3	15.24	−0.40
Q.FLS.hnau-3BS	E1	Mar207	Mar289	14	8.8–12.4	24.5	64.22	−0.99
	E2	Mar207	Mar289	13	8.8–12.4	28.3	68.56	−1.13
	E3	Mar207	Mar289	15	8.8–12.4	17.8	31.44	−0.94
	E4	Mar207	Mar289	14	8.8–12.4	23.8	52.46	−1.29
	E5	Mar207	Mar289	13	8.8–12.4	20.8	58.47	−0.93
	E6	Mar207	Mar289	13	8.8–12.4	16.9	55.91	−0.87

[a]Physical intervals (Mb) were obtained by blasting Indel flanking gene sequences against the reference genome sequence of Chinese Spring (IWGSC, https://urgi.versailles.inra.fr/blastiwgsc/blast.php)

[b]Phenotypic variance explained by the QTL

[c]Estimated additive effect of the QTL; native values indicated that favorable alleles came from Kofa

[d]E1 to E6, Zhengzhou 2017–2018, Yuanyang 2018–2019, Zhengzhou 2018–2019, Yuangyang 2019–2020, Zhengzhou 2019–2020, and Zhengzhou 2020–2021 seasons, respectively

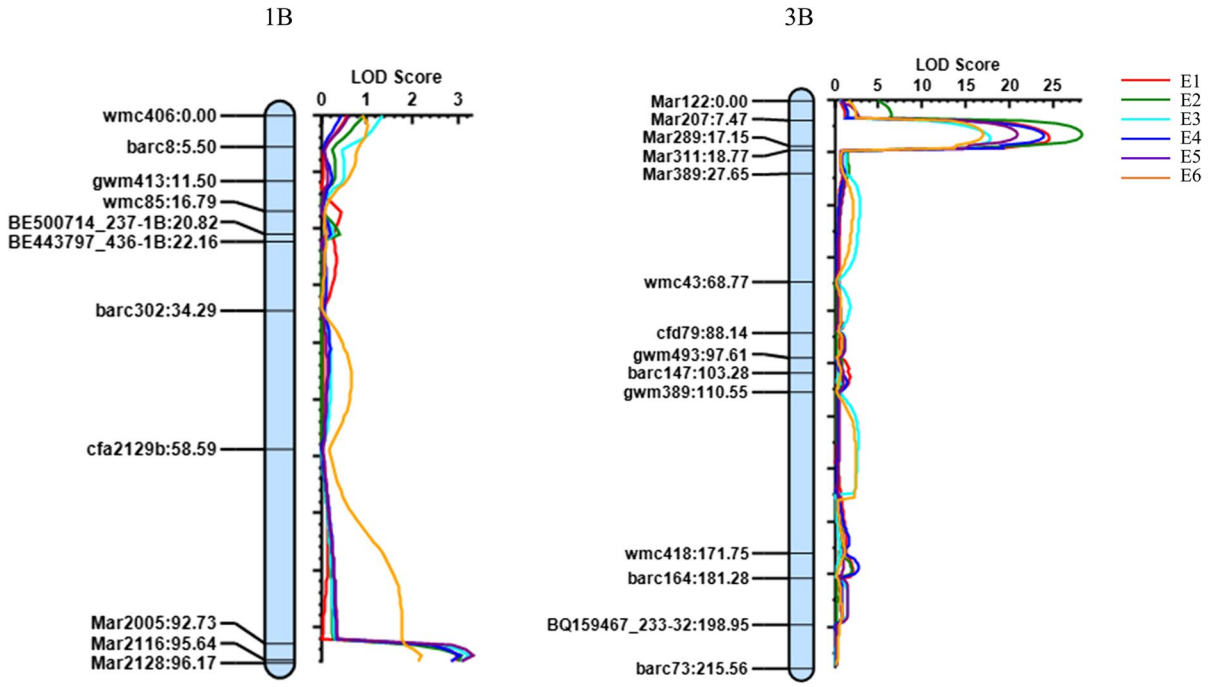

Fig. 4 LOD contours obtained by inclusive composite interval mapping of QTLs for flag leaf senescence in the UC1113/Kofa RIL population. E1 to E6, Zhengzhou 2017–2018, Yuanyang 2018–2019, Zhengzhou 2018–2019, Yuangyang 2019–2020, Zhengzhou 2019–2020, and Zhengzhou 2020–2021 seasons, respectively

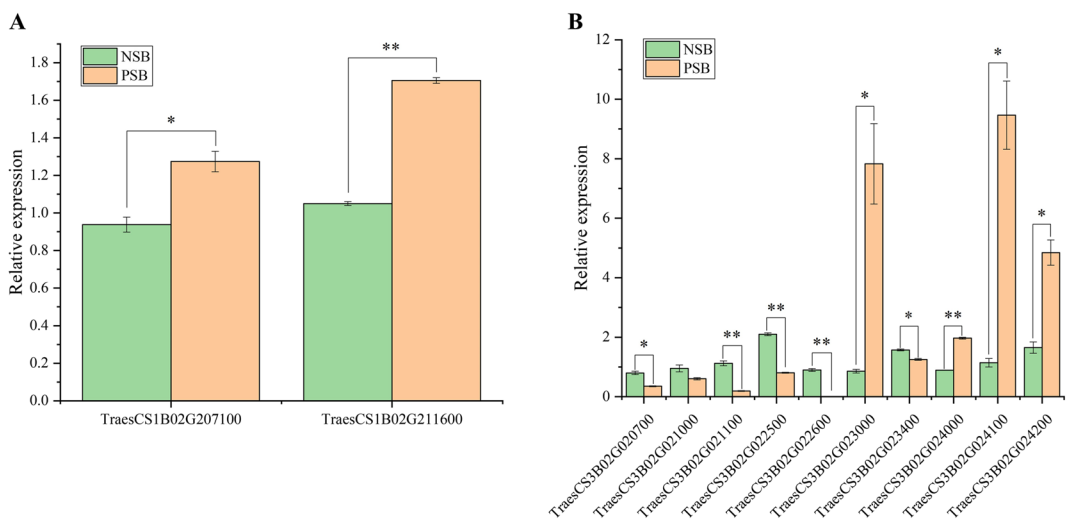

Fig. 5 The relative expression levels of the significant differential genes in NSB and PSB based on qRT-PCR. NSB: normal senescence bulk, PSB: premature senescence bulk. Statistical significance was determined by a two-sided *t*-test (*$P < 0.05$; **$P < 0.01$)

in the Chinese Spring genome. According to BSR-Seq results, 10 of the 82 annotated genes were significantly and differentially expressed between two NSB and two PSB (Table S12). Further analysis of the qRT-PCR analysis showed that the differential expression multiple of TraesCS3B02G023000,

TraesCS3B02G024100, and TraesCS3B02G024200 was significantly higher than other differential genes between normal senescence RILs and premature senescence RILs (Fig. 5B). Expression patterns of these genes in WheatOmics (http://202.194.139.32/) showed that only TraesCS3B02G023000 of the 3 differentially expressed genes was highly expressed in leaf (Table S13). In addition, sequencing results revealed that a SNP (T/C) at 389 bp of TraesCS3B02G023000 resulted in a missense mutation (Leu/Lys) between NSP and PSB. Therefore, TraesCS3B02G023000, annotated as a RING/U-box superfamily protein, was identified as a candidate SAG for *Q.FLS.hnau-3BS*.

Discussion

Since photosynthates in flag leaves contribute about 30% to 50% of assimilates in grains at the post-anthesis stage (Lupton 1966), mapping QTL for FLS and studding the senescence mechanism of flag leaf will help to improve productivity of wheat. Until now, a few of FLS QTLs and molecular markers have been reported in durum and bread wheat. Verma et al. (2004) identified two QTLs for FLS on chromosomes 2B and 2D using amplified fragment length polymorphism (AFLP) and simple sequence repeat (SSR) markers. Barakat et al. (2013) reported one QTL for FLS on chromosome 2D, which was associated with 1 random amplified polymorphic DNA (RAPD) marker, 4 inter-simple sequence repeat (ISSR) markers, and 1 SSR marker. In addition, five QTLs for FLS were identified in an F_4 population of 150 lines derived from Pavon76 and Yecora Rojo using SSR markers (Barakat et al. 2015). In the present study, a UK population with obvious differences of FLS timing was used to identify important genetic loci associated with FLS. To improve the efficiency and cost of marker development and detection, 109 InDel markers were developed on the targeting regions based on resequencing data of bread wheat cultivars from our lab. As is expected, 14 of them were able to find polymorphisms between two NSB and two PSB, indicated a more polymorphic (12.8%) relative to SNP markers (8.4%) (Zhang et al. 2008). Finally, eight new gene-derived InDel markers were added in the targeting region, which here complements the information of genetic map previously reported by Zhang et al. (2008). More importantly, these gene-derived markers can be used as anchor points for comparative studies with the sequenced genomes of wheat.

Our study found that although FLS timing in both parents was normal, but the F_{10} of RILs segregated in a 9 normal: 7 premature senescence ratios (Table S14), indicating the existence of important genetic loci associated with FLS. Using the BSA-wheat 660K array, BSR-Seq, genetic linkage map, and ICIM, two major QTLs for FLS were rapidly mapped on chromosomes 1B and 3B. The *Q.FLS.hnau-1BL* carried normal FLS allele from the tetraploid durum wheat Kofa and was located at 359.2–385.2 Mb with the PVE of 14.2–15.4%. Barakat et al. (2015) identified a QTL on chromosome 1B in the Mexican wheat cultivar Pavon76 that was linked to SSR marker barc194, explaining 21% of phenotypic variances. Because pedigree analyses showed no relationship between Pavon76 and Kofa, *Q.FLS.hnau-1BL* is likely different from the QTL. In addition, compared with the large range of the QTL on 1B from Pavon76, *Q.FLS.hnau-1BL* was greatly narrowed down to a 2.9 cM small interval. Since no QTLs for FLS have been identified previously on chromosome 3BS, *Q.FLS.hnau-3BS* is also possibly a new QTL for FLS. These two QTL and their tightly linked markers could be used in further FLS genes cloning and wheat molecular breeding.

Zhang et al. (2008) reported a strong QTL for grain protein content (GPC), wet gluten content (WGC), and cooked firmness (CFN) on the short arm of chromosome 3B (~7.1–18.8 Mb region in Chinese Spring) in the UK mapping population. Interestingly, *Q.FLS.hnau-3BS* affecting FLS in the study overlaps with the above QTLs for GPC, WGC, and CFN, suggesting that these multiple traits were either the pleiotropic effects of a single gene or the result of multiple independent genes. In previous studies, the high protein content gene *Gpc-B1* showed a relationship with leaf senescence and pleiotropic effects on wheat Zn and Fe content (Uauy et al. 2006a, 2006b). In the present study, we investigated grain size in 2020–2021 cropping season and found that wheat lines containing *Q.FLS.hnau-1BL* and *Q.FLS.hnau-3BS* exhibited significantly higher grain width, grain length, and thousand-grain weight, possibly implying that the delay of FLS increased grain size and weight (Fig. S4). Therefore, mining QTLs and screening candidate

genes that regulate FLS is important for improving wheat yield and grain quality.

Collinearity analysis showed that a high level of collinearity of the *Q.FLS.hnau-1BL* and *Q.FLS.hnau-3BS* genomic regions between *T. aestivum cv.* Chinese Spring and *T. turgidum* ssp. *durum cv.* Svevo (Fig. S5). The assembled genome size of Chinese Spring (IWGSC RefSeq v1.0) was 14.5 Gb, with the scaffolds with N50s of 7.0 Mb (IWGSC 2018). By comparison, the scaffold N50 length for Svevo was 6.0 Mb, and the high-confidence (HC) gene number in the candidate regions for Svevo (175 HC genes) was fewer than that in Chinese Spring (190 HC genes). Consequently, Chinese Spring reference genome (IWGSC RefSeq v1.0) was finally used to screen candidate genes within the two localization regions.

Based on BSR-Seq, qRT-PCR analysis, and gene sequencing, we selected TraesCS3B02G023000 as candidate SAGs for *Q.FLS.hnau-3BS*. By searching homologous genes in WheatOmics database (http://202.194.139.32/), TraesCS3B02G023000 is highly homologous with rice RING-H2 type E3 ubiquitin ligase (Table S15). E3 ubiquitin ligase plays an important regulatory role in the transfer of the ubiquitin to proteins and targeting substrates to the 26S proteasome (Glickman and Ciechanover 2002). Functional studies have identified a number of RING-type E3 ligases as regulators of plant immunity. For example, Wang et al. (2017) reported that RING-H2-type E3 gene *VpRH2* from *Vitis pseudoreticulata* improves resistance to powdery mildew by interacting with VpGRP2A. Recently, Bi et al. (2023) showed that RING-H2 gene OsRFPH2-6 negatively regulated rice immunity against *M. oryzae* and chitin-triggered PTI. The function of TraesCS3B02G023000 also requires more evidence to be confirmed. Our results provide a theoretical basis for fine mapping and functional gene cloning of *Q.FLS.hnau-3BS*.

Using the same methods, TraesCS1B02G211600, located at ~385 Mb, was as a candidate SAG for the QTL on 1B. By searching homologous genes in WheatOmics database (http://202.194.139.32/), TraesCS1B02G211600 is highly homologous with cell wall-associated kinase (WAK) of *Arabidopsis* and rice (Table S16). The WAK gene encodes functional proteins associated with the cell wall and belongs to an important receptor-like protein kinase subfamily in plants (Wang et al. 2012). WAKs, as receptors for signaling molecules, have been recently found to be essential mediators of innate resistance to specific fungal pathogens by ROS control (Li et al. 2020a; Wang et al. 2023). However, the role of TraesCS1B02G211600 in leaf senescence awaits verification and unraveling.

Conclusions

In the study, we identified two novel and major QTLs associated with FLS based on the BSA-wheat 660K array, BSR-Seq, genetic linkage map, and ICIM. Interestingly, *Q.FLS.hnau-3BS* overlaps with the QTL for grain protein content, wet gluten content, and cooked firmness, suggesting a pleiotropic locus associated with grain quality. In addition, we screened two candidate genes in the *Q.FLS.hnau-1BL* and *Q.FLS.hnau-3BS* interval and further analyzed their gene sequence and expression in the RILs in UC1113/ Kofa population. Our finding will provide available molecular markers for wheat breeding and provide a reference for cloning senescence-associated genes, understanding the genetic mechanism of leaf senescence in wheat.

Acknowledgements We thank Dr. Chaonan Shi in the College of Agronomy, Henan Agricultural University, for helping in phenotypic identification.

Author contribution Yan Ren: BSA-wheat 660K array and BSR-Seq analysis and writing—original draft. Xiaonan Sun, Jingyun Nie, and Xiaohui Wu: phenotyping, sampling, and marker development. Peng Guo and Yixiao Zhang: data curation and software analysis. Xia Yang, Congwei Sun, and Ning Zhang: experimental methods and guidance. Mohsin Niaz: modification language. Feng Chen: project administration, writing—review and editing, and funding acquisition.

Funding The research was supported by the National Natural Science Foundation of China (U1904109 and 31861143008), the National Key Research and Development Program of China (2022YFD1201504 and 2019YFE0118300), Henan Major Science and Technology Project (201300111600), and Postdoctoral Science Foundation of China.

Data availability The datasets generated during and/or analyzed during the current study are available on request.

Declarations

Ethics approval and consent to participate Not applicable.

Consent for publication Not applicable.

Conflict of interests The authors declare no competing interests.

References

Barakat M, Saleh M, Al-Doss A, Moustafa K, Elshafei A, AI-Qurainy F. (2015) Identification of new SSR markers linked to leaf chlorophyll content, flag leaf senescence and cell membrane stability traits in wheat under water stressed condition. Aust J Crop Sci. 66(1):93–102. https://doi.org/10.1556/ABiol.66.2015.1.8

Barakat MN, Wahba LE, Milad SI (2013) Molecular mapping of QTLs for wheat flag leaf senescence under water-stress. Biol Plantarum 57(1):79–84. https://doi.org/10.1007/s10535-012-0138-7

Baurley JW, Edlund CK, Pardamean CI, Conti DV, Bergen AW (2016) Smokescreen: a targeted genotyping array for addiction research. BMC Genom 17:145. https://doi.org/10.1186/s12864-016-2495-7

Beers EP, McDowell JM (2001) Regulation and execution of programmed cell death in response to pathogens, stress and developmental cues. Curr Opin Plant Biol 4(6):561–567. https://doi.org/10.1016/S1169-5266(00)00216-8

Bi Y, Wang H, Yuan X, Yan Y, Li D, Song F (2023) The NAC transcription factor ONAC083 negatively regulates rice immunity against Magnaporthe oryzae by directly activating transcription of the RING-H2 gene OsRFPH2-6. J Integr Plant Biol 65(3):854–875. https://doi.org/10.1111/jipb.13399

Cakmak I, Pfeiffer WH, McClafferty B (2010) Biofortification of durum wheat with zinc and iron. Cereal Chem 87:10–20. https://doi.org/10.1094/CCHEM-87-1-0010

Chen F, Xu HX, Zhang FY, Xia XC, He ZH, Wang DW, Dong ZD, Zhan KH, Cheng XY, Cui DQ (2011) Physical mapping of puroindoline b-2 genes and molecular characterization of a novel variant in durum wheat (Triticum turgidum L.). Mol Breeding 28:153–161. https://doi.org/10.1007/S9032-010-9469-2

Cohen M, Hertweck K, Itkin M, Malitsky S, Dassa B, Fischer AM, Fluhr R (2022) Enhanced proteostasis, lipid remodeling, and nitrogen remobilization define barley flag leaf senescence. J Exp Bot 73(19):6816–6837. https://doi.org/10.1093/jxb/erac329

Distelfeld A, Avni R, Fischer AM (2014) Senescence, nutrient remobilization, and yield in wheat and barley. J Exp Bot 65(14):3783–3798. https://doi.org/10.1093/jxb/ert477

Dong C, Zhang L, Chen Z, Xia C, Gu Y, Wang J, Li D, Xie Z, Zhang Q, Zhang X, Gui L, Liu X, Kong X (2020) Combining a new exome capture panel with an effective varB-Score algorithm accelerates BSA-based gene cloning in wheat. Front Plant Sci 11:1249. https://doi.org/10.3389/fpls.2020.01249

Dvorak J, Akhunov ED, Akhunov AR, Deal KR, Luo MC (2006) Molecular characterization of a diagnostic DNA marker for domesticated tetraploid wheat provides evidence for gene flow from wild tetraploid wheat to hexaploid wheat. Mol Biol Evol 23(7):1386–1396. https://doi.org/10.1093/molbev/msl004

Gan S, Amasino RM (1995) Inhibition of leaf senescence by autoregulated production of cytokinin. Science 270(5244):1986–1988. https://doi.org/10.1126/science.270.5244.1986

Glickman MH, Ciechanover A (2002) The ubiquitin-proteasome proteolytic pathway: destruction for the sake of construction. Physiol Rev 82(2):373–428. https://doi.org/10.1152/physrev.00027.2001

Guo Y, Gan S (2005) Leaf senescence: signals, execution, and regulation. Curr Top Dev Biol. 71:83–112. https://doi.org/10.1016/S0070-2153(05)71003-6

Hill JT, Demarest BL, Bisgrove BW, Gorsi B, Su YC, Yost HJ (2013) MMAPPR: mutation mapping analysis pipeline for pooled RNA-seq. Genome Res 23(4):687–697. https://doi.org/10.1101/gr.146936.112

Hörtensteiner S, Feller U (2002) Nitrogen metabolism and remobilization during senescence. J Exp Bot 53(370):927–937. https://doi.org/10.1093/jexbot/53.370.927

Hu Y, Jiang Y, Han X, Wang H, Pan J, Yu D (2017) Jasmonate regulates leaf senescence and tolerance to cold stress: crosstalk with other phytohormones. J Exp Bot 68(6):1361–1369. https://doi.org/10.1093/jxb/erx004

International Wheat Genome Sequencing Consortium (IWGSC) (2018) Shifting the limits in wheat research and breeding using a fully annotated reference genome. Science 361(6403):eaar7191. https://doi.org/10.1126/science.aar7191

Kim J, Woo HR, Nam HG (2016) Toward systems understanding of leaf senescence: an integrated multi-omics perspective on leaf senescence research. Mol Plant 9(6):813–825. https://doi.org/10.1016/j.molp.2016.04.017

Lei L, Wu D, Cui C, Gao X, Yao Y, Dong J, Xu L, Yang M (2022) Transcriptome analysis of early senescence in the post-anthesis flag leaf of wheat (Triticum aestivum L.). Plants (Basel) 11(19):2593. https://doi.org/10.3390/plants11192593

Leng Y, Ye G, Zeng D (2017) Genetic dissection of leaf senescence in rice. Int J Mol Sci 18(2):2686. https://doi.org/10.3390/ijms18122686

Li H, Hua L, Rouse MN, Li T, Pang S, Bai S, Shen T, Luo J, Li H, Zhang W, Wang X, Dubcovsky J, Chen S (2021) Mapping and characterization of a wheat stem rust resistance gene in durum wheat "Kronos". Front Plant Sci 12:751398. https://doi.org/10.3389/fpls.2021.751398

Li Q, Hu A, Qi J, Dou W, Qin X, Zou X, Xu L, Chen S, He Y (2020a) CsWAKL08, a pathogen-induced wall-associated receptor-like kinase in sweet orange, confers resistance to citrus bacterial canker via ROS control and JA signaling. Hortic Res 7:42. https://doi.org/10.1038/s41438-020-0263-y

Li Q, Hu R, Guo Z, Wang S, Gao C, Jiang Y, Tang J, Yin G (2022) SNP-based identification of QTL for resistance to black point caused by Bipolaris sorokiniana in bread wheat. Crop J 10(3):767–774. https://doi.org/10.1016/j.cj.2021.09.007

Li Z, Zhang Y, Zou D, Zhao Y, Wang HL, Zhang Y, Xia X, Luo J, Guo H, Zhang Z (2020b) LSD 3.0: a comprehensive resource for the leaf senescence research community. Nucleic Acids Res 48(D1):D1069–D1075. https://doi.org/10.1093/nar/gkz898

Liang C, Zheng G, Li W, Wang Y, Hu B, Wang H, Wu H, Qian Y, Zhu XG, Tan DX, Chen SY, Chu C (2015) Melatonin delays leaf senescence and enhances salt stress tolerance in rice. J Pineal Res 59(1):91–101. https://doi.org/10.1111/jpi.12243

Lim PO, Kim HJ, Nam HG (2007) Leaf Senescence. Annu Rev Plant Biol 58:115–136. https://doi.org/10.1146/annurev.arplant.57.032905.105316

Liu YX, Tao Y, Wang ZQ, Guo QL, Wu FK, Yang XL, Deng M, Ma J, Chen GD, Wei YM, Zheng YL (2018) Identification of QTL for flag leaf length in common wheat and their pleiotropic effects. Mol Breed 38(1):1–11. https://doi.org/10.1007/s11032-017-0766-x

Livak KJ, Schmittgen TD (2001) Analysis of relative gene expression data using real-time quantitative PCR and the 2(-Delta Delta C(T)) method. Methods 25(4):402–408. https://doi.org/10.1006/meth.2001.1262

Lupton FGH (1966) Translocation of photosynthetic assimilates in wheat. Ann Appl Biol 57(3):355–364. https://doi.org/10.1111/j.1744-7348.1966.tb03829.x

Lv G, Tian Q, Zhang F, Chen J, Niaz M, Liu C, Hu H, Sun C, Chen F (2021) Reduced expression of lipoxygenase genes improves flour processing quality in soft wheat. J Exp Bot 72(18):6247–6259. https://doi.org/10.1093/jxb/erab264

Mu J, Huang S, Liu S, Zeng Q, Dai M, Wang Q, Wu J, Yu S, Kang Z, Han D (2019) Genetic architecture of wheat stripe rust resistance revealed by combining QTL mapping using SNP-based genetic maps and bulked segregant analysis. Theor Appl Genet 132(2):443–455. https://doi.org/10.1007/s00122-018-3231-2

Olsen AN, Ernst HA, Leggio LL, Skriver K (2005) NAC transcription factors: structurally distinct, functionally diverse. Trends Plant Sci 10(2):79–87. https://doi.org/10.1016/j.tplants.2004.12.010

Qu X, Li C, Liu H, Liu J, Luo W, Xu Q, Tang H, Mu Y, Deng M, Pu Z, Ma J, Jiang Q, Chen G, Qi P, Jiang Y, Wei Y, Zheng Y, Lan X, Ma J (2022) Quick mapping and characterization of a co-located kernel length and thousand-kernel weight-related QTL in wheat. Theor Appl Genet 135(8):2849–2860. https://doi.org/10.1007/s00122-022-04154-4

Rushton PJ, Somssich IE, Ringler P, Shen QJ (2010) WRKY transcription factors. Trends Plant Sci 15(5):247–258. https://doi.org/10.1016/j.tplants.2010.02.006

Takagi H, Abe A, Yoshida K, Kosugi S, Natsume S, Mitsuoka C, Uemura A, Utsushi H, Tamiru M, Takuno S, Innan H, Cano LM, Kamoun S, Terauchi R (2013) QTL-seq: rapid mapping of quantitative trait loci in rice by whole genome resequencing of DNA from two bulked populations. Plant J. 74(1):174–183. https://doi.org/10.1111/tpj.12105

Uauy C, Brevis JC, Dubcovsky J (2006a) The high grain protein content gene Gpc-B1 accelerates senescence and has pleiotropic effects on protein content in wheat. J Exp Bot 57(11):2785–2794. https://doi.org/10.1093/jxb/erl047

Uauy C, Distelfeld A, Fahima T, Blechl A, Dubcovsky J (2006b) A NAC gene regulating senescence improves grain protein, zinc, and iron content in wheat. Science 314(5803):1298–1301. https://doi.org/10.1126/science.1133649

Verma V, Foulkes MJ, Worland AJ, Sylvester-bradley CPDS, Snape JW (2004) Mapping quantitative trait loci for flag leaf senescence as a yield determinant in winter wheat under optimal and drought-stressed environments. Euphytica 135:255–263. https://doi.org/10.1023/B:EUPH.0000013255.31618.14

Wang D, Qin L, Wu M, Zou W, Zang S, Zhao Z, Lin P, Guo J, Wang H, Que Y (2023) Identification and characterization of WAK gene family in Saccharum and the negative roles of ScWAK1 under the pathogen stress. Int J Biol Macromol 224:1–19. https://doi.org/10.1016/j.ijbiomac.2022.11.300

Wang L, Xie X, Yao W, Wang J, Ma F, Wang C, Yang Y, Tong W, Zhang J, Xu Y, Wang X, Zhang C, Wang Y (2017) RING-H2-type E3 gene VpRH2 from Vitis pseudoreticulata improves resistance to powdery mildew by interacting with VpGRP2A. J Exp Bot 68(7):1669–1687. https://doi.org/10.1093/jxb/erx033

Wang N, Huang HJ, Ren ST, Li JJ, Sun Y, Sun DY, Zhang SQ (2012) The rice wall-associated receptor-like kinase gene OsDEES1 plays a role in female gametophyte development. Plant Physiol 160(2):696–707. https://doi.org/10.1104/pp.112.203943

Wang S, Wong D, Forrest K, Allen A, Chao S, Huang BE, Maccaferri M, Salvi S, Milner SG, Cattivelli L, Mastrangelo AM, Whan A, Stephen S, Barker G, Wieseke R, Plieske J, International Wheat Genome Sequencing Consortium, Lillemo M, Mather D et al (2014) Characterization of polyploid wheat genomic diversity using a high-density 90,000 single nucleotide polymorphism array. Plant Biotechnol J 12(6):787–796. https://doi.org/10.1111/pbi.12183

Woo HR, Kim HJ, Lim PO, Nam HG (2019) Leaf senescence: systems and dynamics aspects. Annu Rev Plant Biol 70:347–376. https://doi.org/10.1146/annurev-arplant-050718-095859

Woo HR, Kim HJ, Nam HG, Lim PO (2013) Plant leaf senescence and death-regulation by multiple layers of control and implications for aging in general. J Cell Sci 126(21):4823–4833. https://doi.org/10.1242/jcs.109116

Woo HR, Koo HJ, Kim J, Jeong H, Yang JO, Lee IH, Jun JH, Choi SH, Park SJ, Kang B, Kim YW, Phee BK, Kim JH, Seo C, Park C, Kim SC, Park S, Lee B, Lee S et al (2016) Programming of plant leaf senescence with temporal and inter-organellar coordination of transcriptome in Arabidopsis. Plant Physiol 171(1):452–467. https://doi.org/10.1104/pp.15.01929

Xiong EH, Li Z, Zhang C, Zhang J, Liu Y, Peng T, Chen Z, Zhao Q (2021) A study of leaf-senescence genes in rice based on a combination of genomics, proteomics and bioinformatics. Brief Bioinform 22(4):1–35. https://doi.org/10.1093/bib/bbaa305

Zhang HZ, Xie JZ, Chen YX, Liu X, Wang Y, Yan SH, Yang ZS, Zhao H, Wang XC, Jia LH, Cao TJ, Liu ZY (2017) Mapping stripe rust resistance gene YrZM103 in wheat cultivar Zhengmai 103 by BSR-Seq. Acta Agron Sin 43:1643–1649 (in Chinese with English abstract)

Zhang W, Chao S, Manthey F, Chicaiza O, Brevis JC, Echenique V, Dubcovsky J (2008) QTL analysis of pasta quality using a composite microsatellite and SNP map of durum wheat. Theor Appl Genet 117(8):1361–1377. https://doi.org/10.1007/s00122-008-0869-1

Zhao D, Yang L, Xu K, Cao S, Tian Y, Yan J, He Z, Xia X, Song X, Zhang Y (2020) Identification and validation of genetic loci for tiller angle in bread wheat. Theor Appl Genet 133(11):3037–3047. https://doi.org/10.1007/s00122-020-03653-6